

TECHNICAL REPORT 1853  
April 2001

# Optically Controlled Pin-Diode RF Switching for Tactical Signal Intelligence Technology

E. W. Jacobs  
C. K. Sun  
R. Nguyen  
D. Fogliatti  
H. Nguyen  
R. Hunt

**SSC San Diego**

D. J. Albares  
C. T. Chang  
**RF Microsystems, Inc.**

Approved for public release;  
distribution is unlimited.



SSC San Diego  
San Diego, CA 92152-5001

20010823 007

**SSC SAN DIEGO**  
**San Diego, California 92152-5001**

---

---

**Ernest L. Valdes, CAPT, USN**  
**Commanding Officer**

**R. C. Kolb**  
**Executive Director**

**ADMINISTRATIVE INFORMATION**

The work described in this report was performed for Space and Naval Warfare Systems Command (PMW-163) by the Optoelectronics Branch, SSC San Diego from 1 January 1998 to 29 September 2000. Funding was provided under program element 0305885G.

Released by  
S. A. Pappert, Head  
Optoelectronics Branch

Under authority of  
D. M. Gookin, Head  
Networks and Information  
Systems Division

## EXECUTIVE SUMMARY

### OBJECTIVE

The Tactical Signal Intelligence (SIGINT) Technology (TST) program objective was to develop optically controlled PIN-diode radio frequency (RF) switches and demonstrate their feasibility to enhance electromagnetic interference (EMI) immunity, sensitivity, speed, and reliability in front-end SIGINT systems.

### APPROACH

Project members performed the following tasks to reach the project objective:

- Surveyed, analyzed, and selected U.S. Army, Air Force, and Navy SIGINT systems for optoelectronic (OE) switch development goals.
- Developed switch circuit designs for these applications.
- Developed switch technology to implement these designs and to assess its present performance and limitations.
- Demonstrated feasibility in the laboratory and in SIGINT system equipment where possible.

### RESULTS

The TST Program developed optically controlled PIN-diode-based RF switches for potential TST applications. Applications included EMI immunity, bias-free operation, switching speed, low noise, power handling, and reliability. A U.S. Air Force Common Aperture RF (CARF) and a U.S. Army tactical jammer (TACJAM) system provided performance goals. CARF featured very high ON-OFF ratios at X-band. These ON-OFF ratios were provided by current mechanical switches. TACJAM featured high RF power handling and isolation. For these applications, the TST Program designed, built, and tested switch circuits based upon the photovoltaic (PV)-PIN switch and the PIPINS. For the CARF case, a PV-PIN circuit yielded suitable isolation, but not insertion loss. The shortfall was caused by inherent semiconductor-based switch properties and microwave packaging techniques. For the TACJAM case, which used a T/R switch, the PIPINS circuit reached the performance goals up to 100-W cw (instrument-limited). Single PIPINS later handled 200-W cw in cold switching (instrument-limited) and 175-W cw in hot switching.

The TST Program studied the potential advantages of SIGINT applications for three Services. These applications guided OE switch development. The U.S. Air Force CARF X-band bypass switch and the U.S. Navy Combat Direction Finding (CDF) very high frequency/ultra high frequency (VHF/UHF) commutating antenna feed switch were typical examples of low-power, receive, and RF switching applications. High-power RF switching applications were exemplified in the Army (and Marine Corps) TACJAM VHF/UHF T/R switch. The optical PIN diode switches (OPDS) program accomplished the following tasks:

- Analyzed optical PIN diode switches. The PV-PIN switch (figure 1) is based upon conventional OPDS concepts for TST.
- Assessed commercial off-the-shelf (COTS) and developmental PIN diodes for PIPINS.

- Built and characterized the PIPINS at high RF powers under cold- and hot-switching conditions. Cold switching handled greater than 200-W cw at 333 MHz and was limited by the power amplifier (PA) (previous power level: 20 W). Hot switching reached 175 W at 300 MHz and was limited by latch-on (previously unstudied).
- Developed PIPINS-based T/R switch circuits for TACJAM. A 1 x 2 circuit operated at  $\approx$ 100-W cw (PA limited) over 30 to 225 MHz, reaching the goals of 110 dB Is and 0.8 dB IL (previous multithrow PIPINS circuit power: 10 W).
- Expanded PV-PIN switching to exploit COTS X-band monolithic PIN diode circuits at low power and to control them with PV cells through hybrid integration. A 1 x 3 configuration for the CARF bypass switch was demonstrated with 70 dB Is and  $\approx$ 4 dB IL over 8 to 12 GHz. (compound PV-PIN switch circuits not previously introduced).

# CONTENTS

EXECUTIVE SUMMARY.....	iii
1. INTRODUCTION AND BACKGROUND .....	1
2. OPTICALLY CONTROLLED PIN-DIODE SWITCH DEVELOPMENT .....	3
2.1 LOW-POWER, HIGH-FREQUENCY OPDS DEVELOPMENT .....	4
2.1.1 PIPINS-Based Switch Circuit Development .....	4
2.1.2 PV-PIN-Based Switch Circuit Development.....	5
2.1.3 Measurements.....	9
2.1.4 Discussion.....	9
2.2 HIGH-POWER OPDS DEVELOPMENT .....	11
2.2.1 PIPINS Fabrication and Characterization Up to 200 W.....	11
2.2.2 T/R Switch Circuit Development and Demonstration .....	14
3. SUMMARY.....	21
4. REFERENCES.....	23

## Figures

1. PV-PIN switch circuit diagram showing each PIN diode driven by a PV cell through chokes .....	2
2. Schematic, photograph, and circuit diagram of the PIPINS.....	2
3. Quarter-wave transformer switch using PIPINS for the shunt switches. The IL $\leq 0.3$ dB at 2 to 12 GHz and $I_s = 42$ dB at 2 GHz, 32 dB at 12 GHz .....	5
4. Design of the 1 X 3 switch using series-shunt PIN switches with PV cells for control.....	6
5. PV-PIN-based 1 X 3 switch circuit with channelized waveguides on a Duriod substrate.....	7
6. Packaged switch, laser sources, optical control fibers, and RF cables .....	8
7. (A) Isolation of the PV-PIN-based 1 X 3 switch circuit versus frequency. (B) Insertion loss of the PV-PIN-based 1 X 3 switch circuit versus frequency.....	10
8. Insertion loss of a PIPINS versus input RF power for three frequencies .....	12
9. Hot-switched PIPINS output versus time for a 300-MHz signal.....	13
10. Hot-switched series-shunt PIPINS output (170 W) versus time for a 300-MHz signal (rising and falling edges).....	13
11. Latch-on power versus repetition period where the duty cycle is 50% .....	14
12. T/R switch circuit design using PIPINS series-shunt switches. Top: transmit mode. Bottom: receive mode.....	15
13. Isolation versus frequency for the switch design in figure 12. The data are recorded after 96 dB of amplification. Therefore, isolation at the 225-MHz marker is -125.725 dB ...	17
14. Insertion loss versus frequency for the switch design in figure 12.....	18
15. Insertion loss versus RF power at three frequencies for the switch design in figure 12.....	19
16. Isolation versus input power for the switch design in figure 12 measured in the OFF-state arm with the other arm in the ON-state .....	19

## Table

1. OPDS TST RF switching goals.....	4
-------------------------------------	---



# 1. INTRODUCTION AND BACKGROUND

Military platforms suffer severe antenna crowding. Hundreds of antennas interfere with each other electromagnetically and present space, weight, and cost problems. Broadband systems challenge the efficiency of antenna components. Interference and noise usually limit the handling of low-level signals in radio frequency (RF) transmission and circuits. The relentless push of information requirements, analog and digital, toward ever higher RF system capacity increases these problems.

Optically controlled, optoelectronic (OE) RF switching based upon PIN-diode and field-effect transistor (FET) semiconductor technology offers new approaches to these limitations and problems. Placing an RF switch at the end of a tiny optical fiber, electromagnetically isolated, with or without bias, in a remote environment without perturbing surrounding devices, circuits, antennas, or electromagnetic (EM) fields offers a new dimension to the design of RF microwave equipment. Optically controlled OE RF switches bring this EM-isolated, quiet (low-noise) switching capability within reach. Optically controlled OE RF switches provide the following features:

- Switches and control lines electromagnetically isolated—no EMI: pickup, crosstalk, ground loops
- Surrounding EM fields unperturbed
- Signal and control isolated (within the switch)
- Bias-free operation possible
- Semiconductor speed, power handling, and reliability
- Optical fiber control lines small, lightweight, low-loss (multi-km distances)
- Needs electrical-optical conversion (for switch control)

The Tri-Service Tactical Signal Intelligence (SIGINT) Technology (TST) Program conducted this 3-year, 6.2 technology development and demonstration project that studied SIGINT applications of OE RF switching. After considering the FET switch controlled by voltage from a photovoltaic (PV) cell (PV-FET) (Sun et al., 1996; Albares et al., 1999), we chose two other OE PIN-diode switches for this work: (1) the PIN-diode switch controlled by the PV cell (PV-PIN) (Sun et al., 1999), and (2) the photoinjection back-to-back PIN switch (PIPINS) (Sun et al., 1997; Sun, Nguyen, and Albares, 1998; Sun et al., 1998). These switches are called optical PIN-diode switches (OPDS). The PV-PIN switch (figure 1) is based upon conventional PIN RF switches controlled by current from the optically activated PV cells. The PIPINS (figure 2) is a back-to-back PIN-diode configuration where direct optical injection creates electron hole pairs in the intrinsic (I) region of the diodes, producing the conduction (ON) state. Without illumination, the diodes present a high (capacitive) impedance, producing the OFF-state. SPAWAR Systems Center, San Diego (SSC San Diego), with contractual support from RF Microsystems, Inc., performed the work described in this report.

The TST Program studied and developed OPDS, which generally has the same switching performance as similar PIN-diode-based switches with conventional electrical control. OE switching is different and unique in that optical control offers complete EM isolation, elimination, or reduction of switch parasitics, and in some designs, elimination of bias. Other benefits are listed above. OE switching has added complexity because the control signal must be converted into optical form, usually via a laser diode.

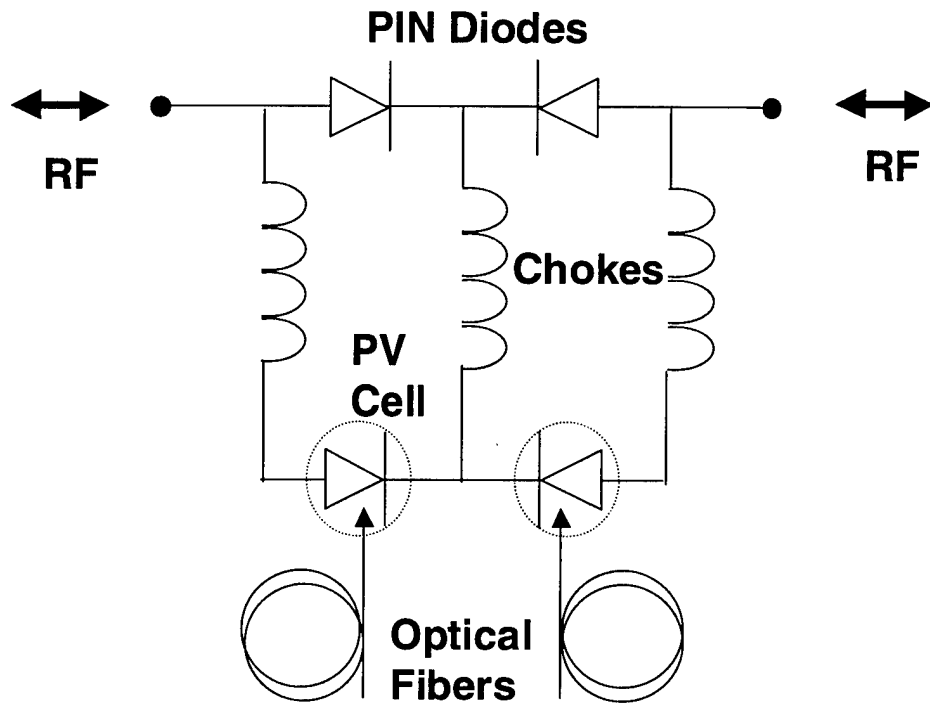


Figure 1. PV-PIN switch circuit diagram showing each PIN diode driven by a PV cell through chokes.

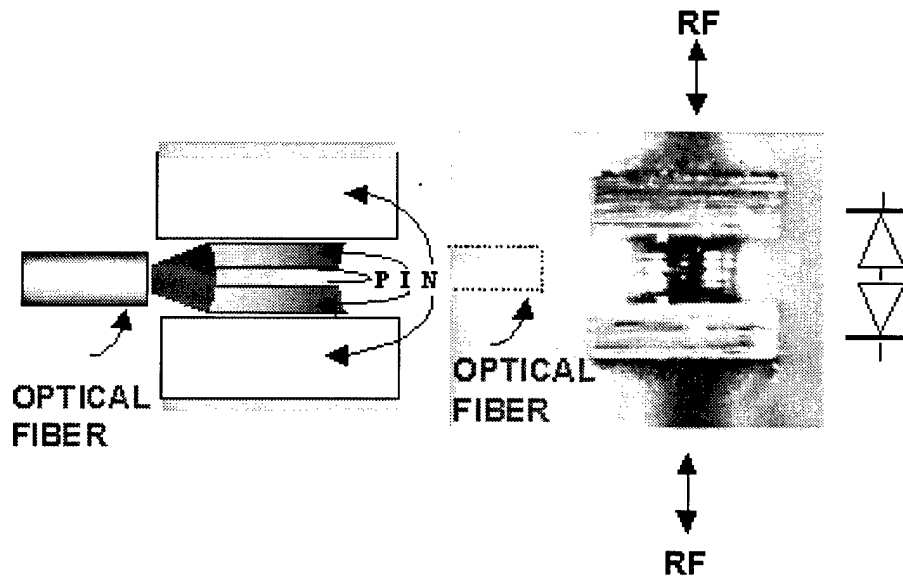


Figure 2. Schematic, photograph, and circuit diagram of the PIPINS.



## 2. OPTICALLY CONTROLLED PIN-DIODE SWITCH DEVELOPMENT

Optically controlled PIN-diode switch development included the following recommendations:

- Investigate the PIPINS device design-fabrication of (1) monolithic vertical structures, and (2) lateral PIN-diode configurations
- Develop accurate large-signal PIPINS models
- Improve RF power handling in the PIPINS. Investigate and develop devices at power levels up to 1 kW

RF switching characteristics vary widely. Nevertheless, the simple series switch model of a variable resistor,  $R_{ON}$  or  $R_{OFF}$ , in parallel with a capacitor,  $C$ , plus transmission line considerations, provide representative device performance. The OFF impedance should be large and the ON impedance should be small. Typical numbers are  $Z_{OFF} = 1/\omega C / 1 \text{ k}\Omega$  and  $R_{ON} .5 \Omega$ . For this case, if the frequency,  $f = 100 \text{ MHz}$ , then  $C .1.7 \text{ pF}$ . Translated to series switching in a  $50\text{-}\Omega$  line, these numbers correspond to isolation,  $(Is) = 20 \text{ dB}$ , and insertion loss,  $(IL) = 0.4 \text{ dB}$ . The parameters,  $Is$  and  $IL$ , are traded off in the series switch, leading to a figure of merit,  $\approx 1/R_{on}C$ .

Naturally switching is performed across the RF spectrum; applications of optically controlled devices range, so far, from about 10 MHz to over 10 GHz. The drop in  $Is$  with frequency can be countered by inductor tuning (if the resulting limited bandwidth is tolerable), or where a ground plane is nearby, such as in a microstrip, by shunt or series-shunt switch designs. Switching antenna radiating elements provide an important example where there may be no local ground plane.

RF power-handling demands are found up to kilowatts peak for radars. Required switching times extend from msec to below  $\mu\text{sec}$ . Naturally minimum control power is sought, particularly for mobile platforms.

The SIGINT systems chosen for potential applications and performance guidance were the Air Force Workstation Prototype Laboratory (WPL) Combat Sent Common Aperture RF (CARF), the Navy (SSC San Diego) Multifunction Electromagnetic Radiation System (MERS), and the Army Communications Electronics Command (CECOM) TACJAM. The Air Force and California Microwave Inc. (CMI) recommended that the Air Force application conducted at CMI be a target for the OPDS Program. The switch, in the CARF part of the Combat Sent aircraft system, is an X-band, low-power,  $1 \times 3$ , high-isolation, low-insertion-loss, low-noise, bypass switch. CMI provided SSC San Diego with performance goals based upon the mechanical switches now used, and provided guidance for the feasibility testing and demonstration of the proposed optically controlled switch. CMI wanted reductions in size, weight, and control power of the mechanical switches. This CARF-related effort concluded at the end of Fiscal Year (FY) 1999.

The Combat Direction Finding (CDF) antenna system, a leading U.S. Navy application planned for incorporation into MERS (a developmental mast enclosure combining several antenna systems) was analyzed. The CDF concept involved sorting received signals from different directions around the horizon by multiple (four to six) antennas. This system connected the antennas with the receiver through a commutating RF switch whose performance would be enhanced by EM isolation and low switching noise, characteristics offered by OE RF switches. Programmable scope and scheduling of MERS eventually deferred this effort, but OE switching for this application appears feasible in light of technology advances.

The Army TACJAM T/R switch (1 x 2) requires high peak power, high isolation, and low insertion loss at UHF or VHF. EMI reduction in the high-power environment was sought. Table 1 lists the goals extracted from these Service applications.

Table 1. OPDS TST RF switching goals.

	Air Force CARF	Navy CDF	Army TACJAM
Configuration	1 x 3	1 x 6	1 x 2
Insertion loss (dB)	0.3	1.0	minimum
Isolation (dB)	60.0	30.0	100.0
Frequency	8 to 12 GHz	500 to 1200 MHz	30 to 225 MHz
RF power	receive	receive	0.2 to 1.0 kW peak
Control power	<3W	minimum	minimum
Switching time	msec	100 $\mu$ sec	-

## 2.1 LOW-POWER, HIGH-FREQUENCY OPDS DEVELOPMENT

Both OPDS types were tried for this switching regime: the PIPINS (figure 1) and the PV-PIN switch (figure 2). PIPINS requires no PV cells, electrical bias, or bias-related isolation circuitry, and its optical-to-electrical conversion is more efficient. Monolithic X-band PIN-diode circuits that approach the CARF switch requirements are COTS. The program preferred the PV-PIN approach because the COTS switches provided much of the stringent microwave packaging. These two approaches for the CARF application are discussed in subsections 2.1.1 and 2.1.2.

### 2.1.1 PIPINS-Based Switch Circuit Development

The first design for the 1 x 3 X-band switch used three PIPINS in each arm of the circuit. Each PIPINS was shunted to ground and separated by a quarter wavelength for impedance transformation; figure 3 shows one pair. Distributed element circuit simulations, on the Serenade Package from Ansoft, showed that this design promised to meet the  $I_s$  target, and to come within  $\approx 1$  dB of the  $I_L$  target. The microstrip circuit was built on 20-mil RT-Duriod, resulting in a geometry convenient for the size of the PIPINS and the length of the quarter-wave transmission lines. The circuit was mounted on a flat plate and connections were made with surface mount assembly (SMA)-type connectors. The performance obtained,  $I_L = 2$  to 4 dB and  $I_s = 38$  to 54 dB, did not reach the simulation predictions or the goals over the 8- to 12-GHz band. We attributed this performance to mismatches in mounting the discrete PIPINS and stray radiation coupling. Careful microwave packaging could reduce these effects.

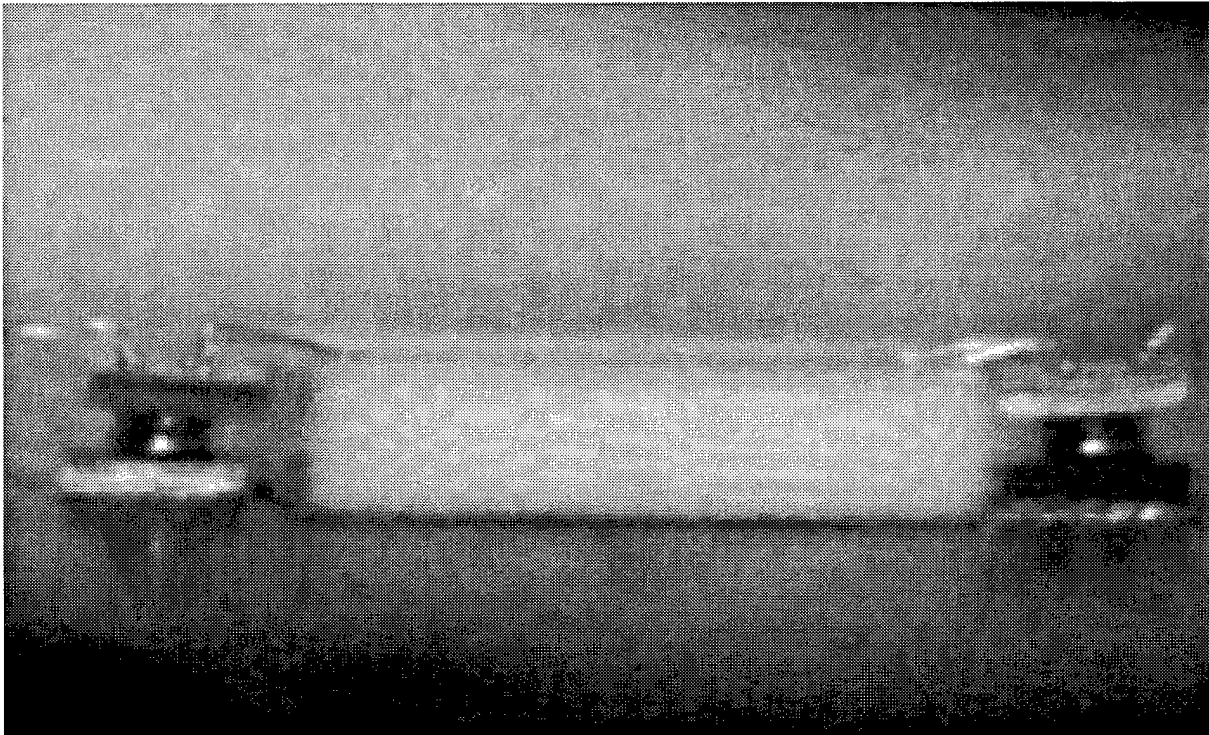


Figure 3. Quarter-wave transformer switch using PIPINS for the shunt switches. The IL  $\leq 0.3$  dB at 2 to 12 GHz and  $I_s = 42$  dB at 2 GHz, 32 dB at 12 GHz.

### 2.1.2 PV-PIN-Based Switch Circuit Development

An approach using COTS-integrated PIN-diode switch circuits and hybrid coupled PV cells took advantage of the added level of monolithic circuit integration with its attendant microwave packaging. Figure 4 shows the design of a 1 x 3 switch using COTS series-shunt PIN switches in combination with PV cells that provided control currents. At the center of figure 4 is a monolithic 1 x 3 series-shunt PIN switch (MACOM #MA4SW310, which costs a few dollars). The  $I_s$  of this switch alone is insufficient, so an additional COTS single series-shunt switch (MACOM #MA4SW110, which costs a few dollars) in a back-to-back configuration was inserted in each arm. The circuit was assembled on a channelized substrate using 5-mil RT-Duroid and Wiltron K-type precision connectors. A laser diode activated each PV cell through an optical fiber. The shunting diodes needed bipolar control to turn the switch ON and OFF. Without these shunting diodes, the back-to-back PV-PIN configuration would yield an OFF-state without biasing, but with insufficient  $I_s$  (Sun et al., 1999). Figure 5 shows a circuit photograph and figure 6 shows one of the switch packages with control fibers and RF cables.

The laser sources used were variable laboratory-type laser diode supplies from Photonic Power Systems (#PPS-700-03) and from RF Power Systems. The PV cells were from Photonic Power Systems. The ON-state biasing used 6-volt PV cells (#PPC-6E-ST) and the OFF-state biasing used 2-volt PV cells (#PPC-2T-ST). The 6-volt cells generated up to  $\approx 40$  mA with 500 mW of optical power while the 2-volt cells required one-third of this optical power to generate the same amount of current.

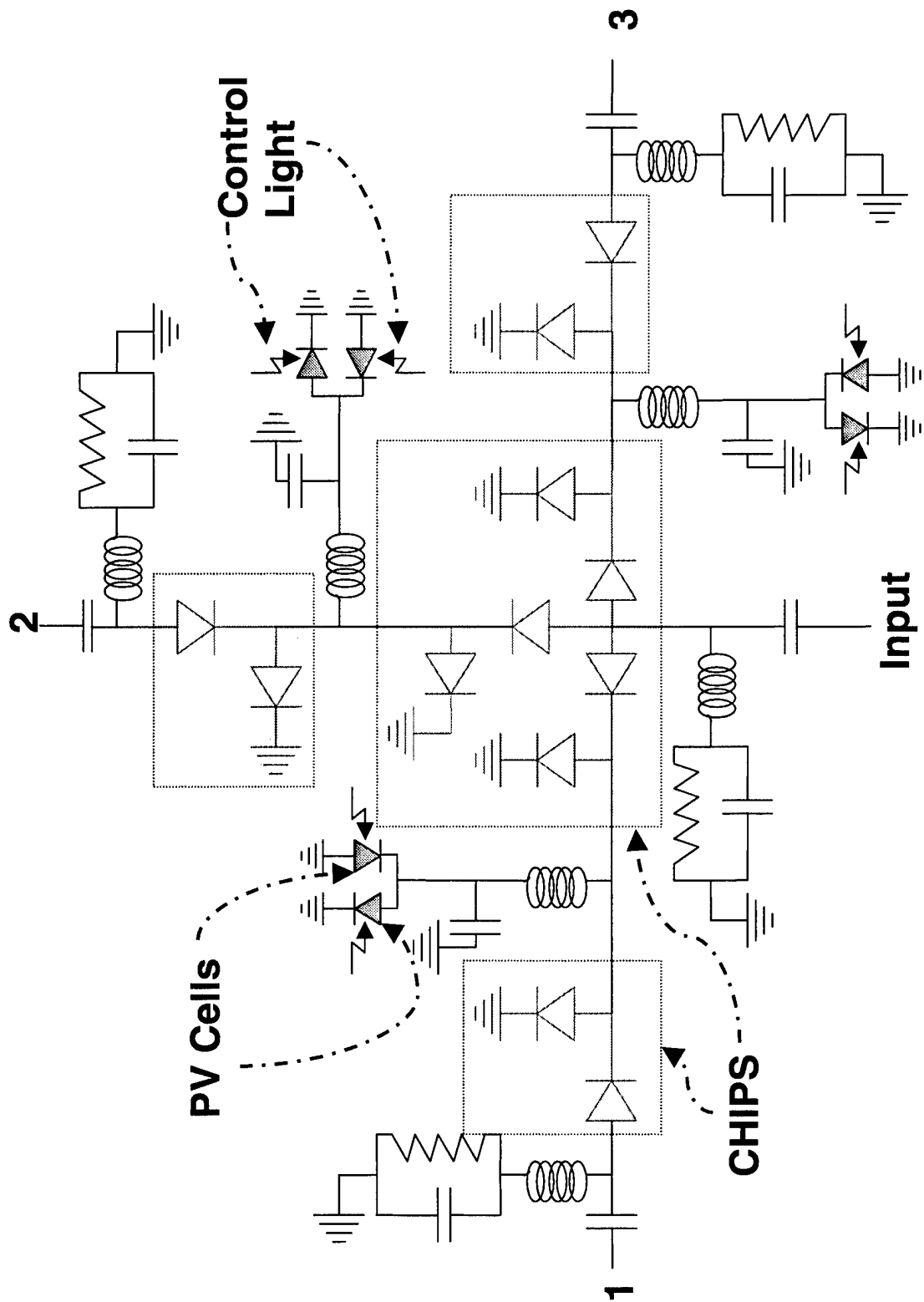


Figure 4. Design of the 1 X 3 switch using series-shunt PIN switches with PV cells for control.

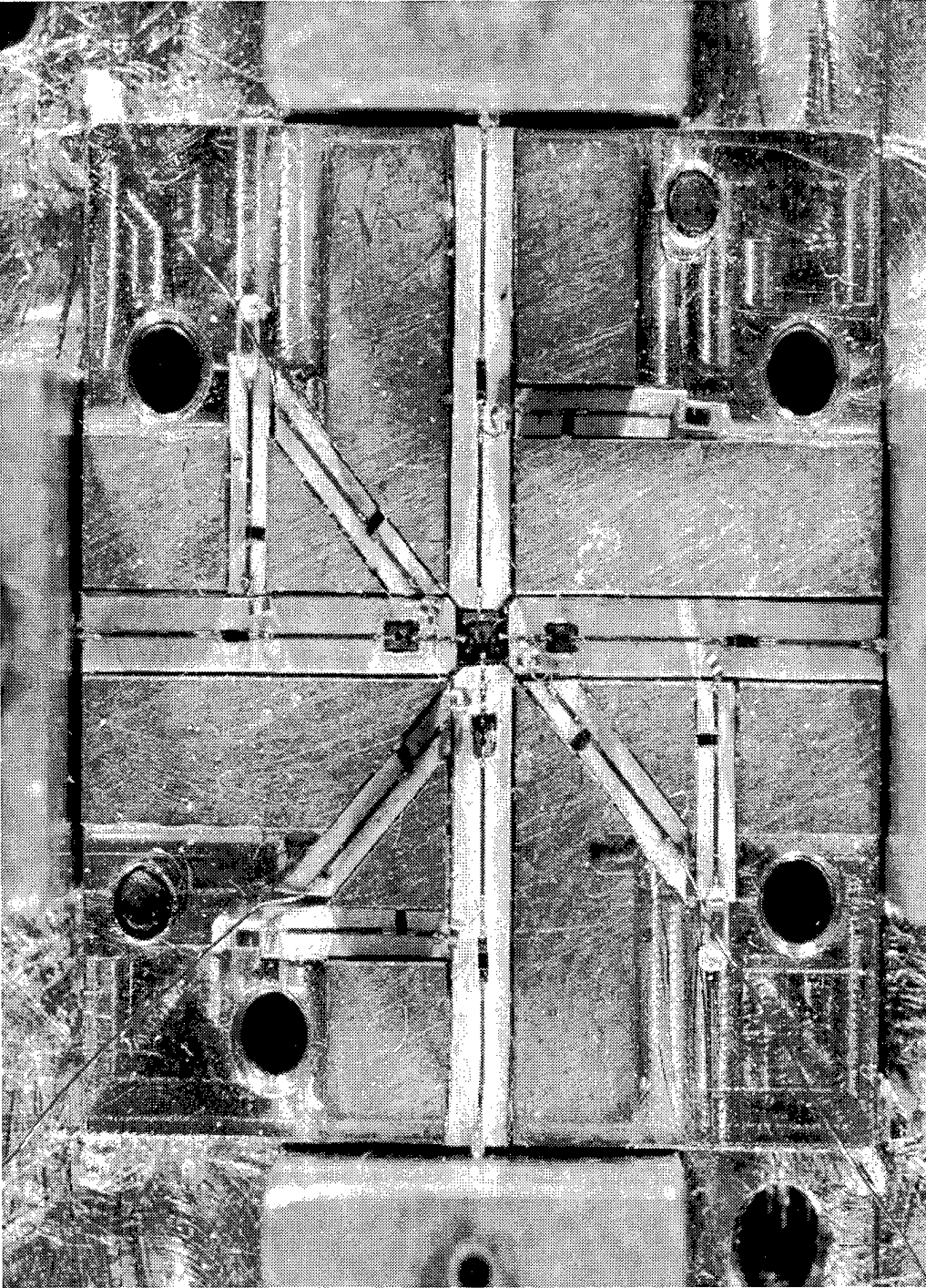


Figure 5. PV-PIN-based 1 X 3 switch circuit with channelized waveguides on a Duriod substrate.

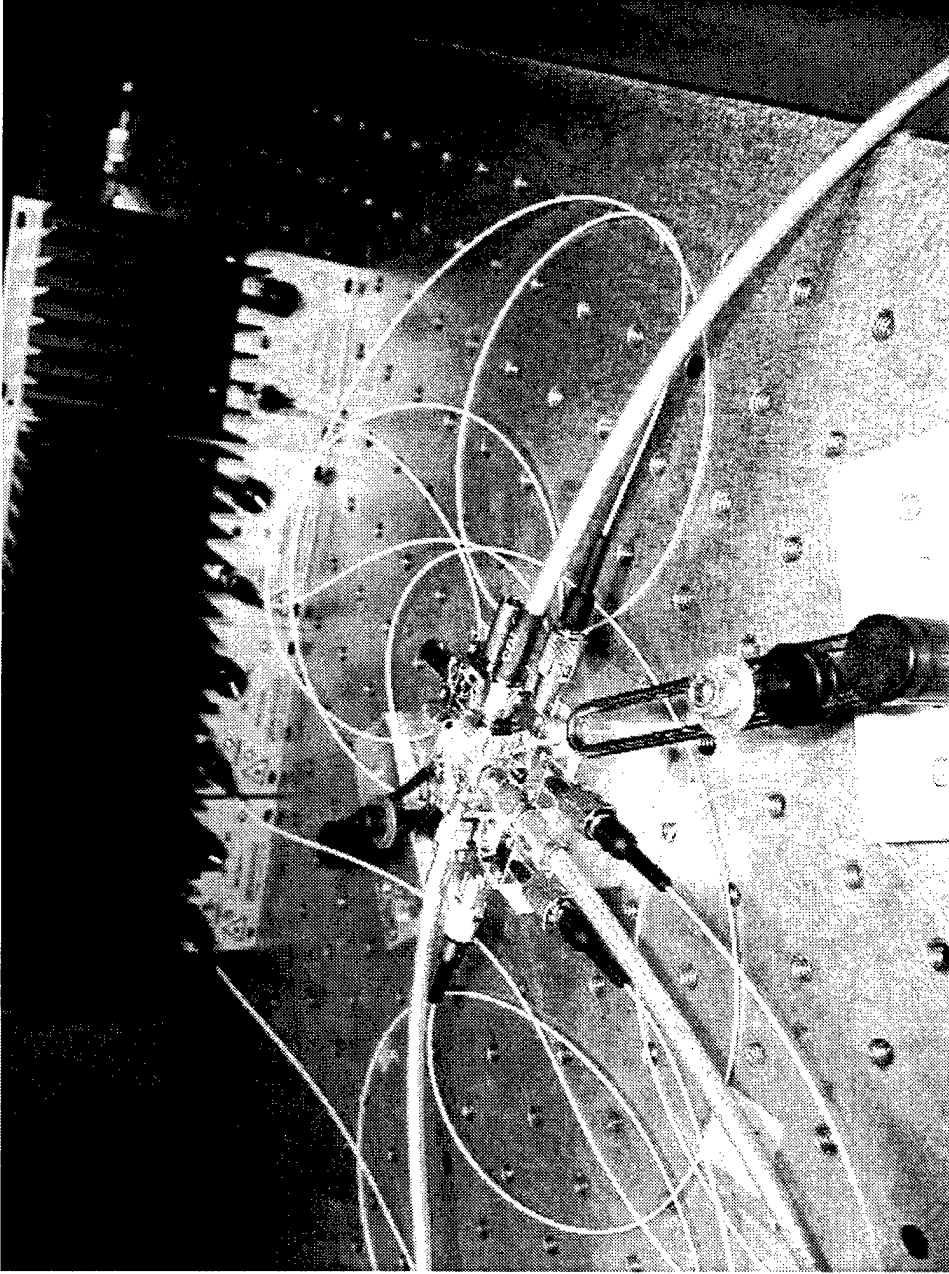


Figure 6. Packaged switch, laser sources, optical control fibers, and RF cables.

### 2.1.3 Measurements

A Hewlett-Packard HP8501 Network Analyzer (0.045 to 50 GHz) measured the  $I_s$  and  $I_L$  of this PV-PIN-based switch. Each arm of the switch was tested individually while the other two arms were terminated in  $50 \Omega$ . Figure 7(A) shows the  $I_s$  measurements with six traces, two for each arm of the switch. One trace for the right arm of the switch is with the center arm ON and the left arm OFF, while the other trace for the right arm is with the center arm OFF and the left arm ON. Data for the center and left arm were taken in a similar fashion, resulting in six traces. So, the  $I_s$  target of 60 dB is exceeded by  $\approx 10$  dB across the 8- to 12-GHz band.

The  $I_L$  measurements were calibrated against a straight-through cable rather than a package similar to the switch package with straight-through transmission lines. This calibration compared the results to that of the currently used mechanical switch that showed a 0.3-dB loss relative to a straight-through cable. So, the  $I_L$  results here include connector loss, transmission line loss, and loss from the switch components and wire bonds. Figure 7(B) shows three traces over the 8- to 12-GHz band, one for each arm in the ON-state, with the other two arms in the OFF-state. The  $I_L$  is  $\approx 3$  to 4 dB above the target of 0.3 dB.

### 2.1.4 Discussion

We estimate that a 1- to 2-dB reduction might be obtained. The COTS switch components alone cause the minimum  $I_L$  and, according to their specifications, is about 1.3 dB (still above the target). The shoulder of a peak in the  $I_L$  curve just above the 8- to 12-GHz band increases the  $I_L$  about 0.5 dB for the right arm of the switch near 12 GHz. This peak can probably be eliminated. The remaining losses could be caused by connections from the transmission lines to the K-type connectors, transmission line loss and mismatches, and bonding wires from the transmission lines to the diode switch components.

Using a single monolithic 1 x 3 diode switch with a series double-shunt on each arm could reduce the  $I_L$  caused by the COTS switches by  $\approx 0.5$  dB. This chip is commercially available, although it is expensive (about \$2000 each in small quantities) and has a long lead-time. (The diode switches used in the present design cost a few dollars each.)

Another consideration is the optical source power. The general-purpose laser diode supplies used in the experiments generate high optical power and need thermoelectric cooling. The PV-PIN-based switches for CARF-type deployment could be designed to use optical power low enough for passive (heat-sink) cooling, making a simpler, lower cost source. For the OFF-state, the current design requires  $\approx 150$  mW of optical power while the ON-state requires  $\approx 500$  mW. Modifying the circuit and the current reduces the optical power requirement for the ON-state close to that of the OFF-state. The single monolithic series double-shunt 1 x 3 switch also takes less optical power. At these power levels, laser diodes cooled only by heat sinks are available. A single unit housing the six laser diodes and associated drive circuitry could be built.

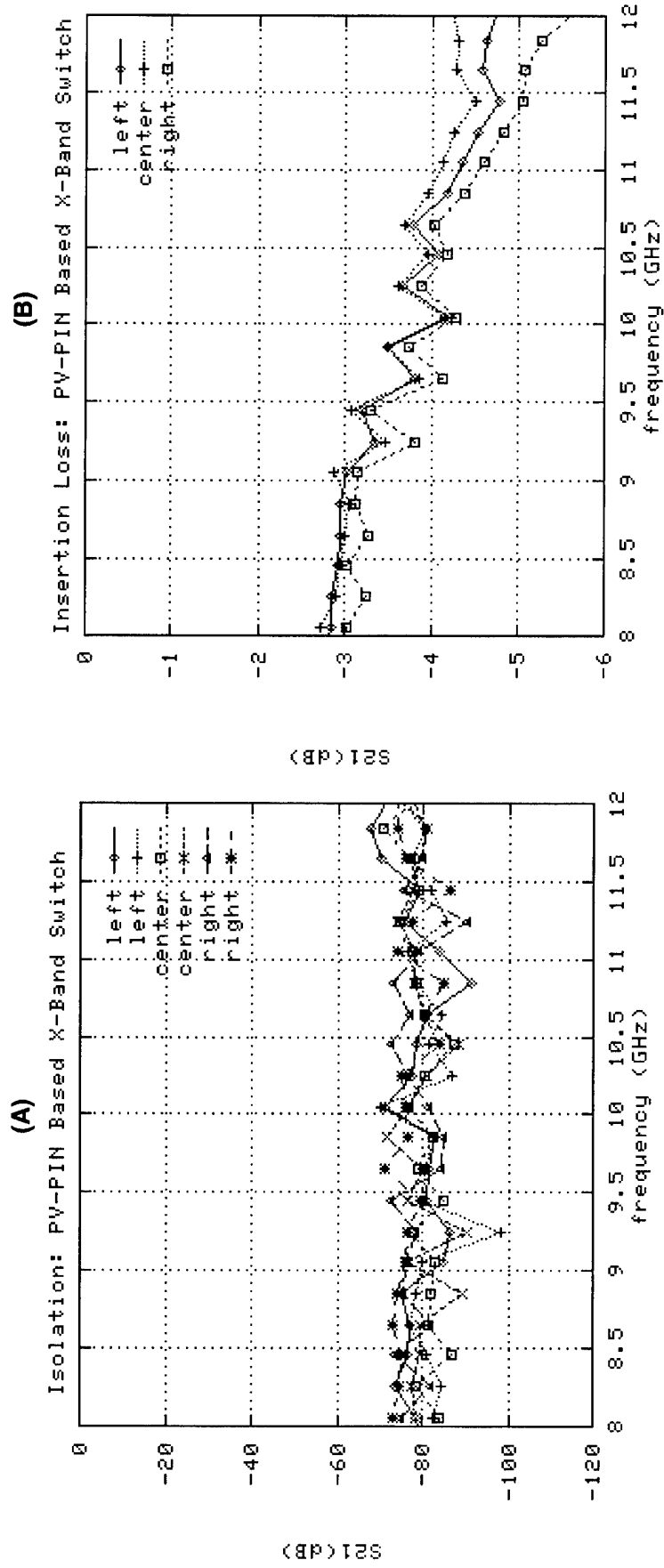


Figure 7. (A) Isolation of the PV-PIN-based 1 X 3 switch circuit versus frequency. (B) Insertion loss of the PV-PIN-based 1 X 3 switch circuit versus frequency.



On 3 August 1999, Air Force contractors from Marconi and Drs. M. St. John and John Gallo visited SSC San Diego. Program status was reviewed and the PV-PIN-based 1 x 3 X-band switch was demonstrated. Although the  $I_s$  was well above the target, because the IL across the 8- to 12-GHz band was 3 to 5 dB short of the 0.3-dB target, testing of this switch in a CARF test bed was not warranted. As discussed above, the IL of this design could be improved upon, though even in the best case estimates, it will probably fall about 2 dB short of the 0.3-dB target. The main advantages of OE switches (e.g., EM-isolation, possible lack of a bias requirement) and semiconductor switches in general (e.g., speed, reliability) were not decisive for this application because the advantages of mechanical switches (IL and  $I_s$  performance) were the most important considerations. So, the CARF-related switching work was concluded.

## 2.2 HIGH-POWER OPDS DEVELOPMENT

The high-power OPDS development effort was made up of two parts: (1) the fabrication and characterization of single PIPINS, and (2) the development of a PIPINS-based TACJAM T/R-type switch circuit. In the PIPINS portion, single PIPINS were built and characterized under cold- and hot-switching conditions at RF powers up to 200-W cw, a power limit set by the procured PA. The circuit portion was a T/R switch circuit design and demonstration that used high-power PIPINS. This T/R switch met the ON-OFF (IL- $I_s$ ) goals listed in table 1. This section discusses these two phases after a note on the TACJAM program.

During FY 1999, the TACJAM program was transferred from the Army to the Marine Corps, while the Army still had objective requirements for TACJAM under the Prophet Air part of the Prophet program. We informed the Marine Corps' TACJAM office about the TST program and continued using CECOM's TACJAM performance goals. Near the end of FY 1999, we learned that the Navy Information Warfare Agency (NIWA) also administers a project with switch requirements similar to TACJAM and briefed NIWA on this program. NIWA expressed interest and said that application development could be included in their outyear planning.

### 2.2.1 PIPINS Fabrication and Characterization Up to 200 W

The PIPINS (figure 2) were made by soldering together the P contacts of two silicon PIN mesa diodes. The epitaxially grown I layer (carrier concentration  $\approx 10^{12}/\text{cm}^3$ ) was either 50- or 100- $\mu\text{m}$  thick, the passivating oxide was transparent, and the mesa diameter was 760  $\mu\text{m}$ .

Both cold switching (where switching occurs when the RF signal is off or at low power) and hot switching (where switching occurs in the presence of high RF power) were studied. Measured characteristics included conversion efficiency, IL, standoff voltage, transition times, latch-on, and linearity (Jacobs et al., 2000).

The PIPINS were characterized for total conversion efficiency ( $\eta_t$ ) of photons to electron/hole pairs versus optical power ( $P_o$ ) incident from the fiber. In this case,  $\eta_t$  accounts for the quantum efficiency of the device and the optical coupling efficiency from the optical fiber to the device. Measurements of  $\eta_t$  ranged from about 0.8 to 0.4 as  $P_o$  increased from 10 to 700 mW. This variation is attributed to increased recombination and electric field screening effects caused by the increasing density of photogenerated charge carriers. An  $\eta_t$  of 0.8 corresponds to a responsivity of  $\approx 0.5$  A/W, typical for OE detectors.

High RF power IL measurements (figure 8) were made with a 200-W cw PA (Ophir GRF5041). The signal was attenuated after the PIPINS (with attenuators rated at 1 kW to reduce error caused by

the change in attenuation caused by heating) before the power was measured with a Hewlett-Packard HP 36A RF power meter. These measurements were calibrated against a package identical to the PIPINS package, but with a straight-through transmission line. These data were taken at  $f = 30, 88,$  and  $333$  MHz with  $P_o = 650$  mW.

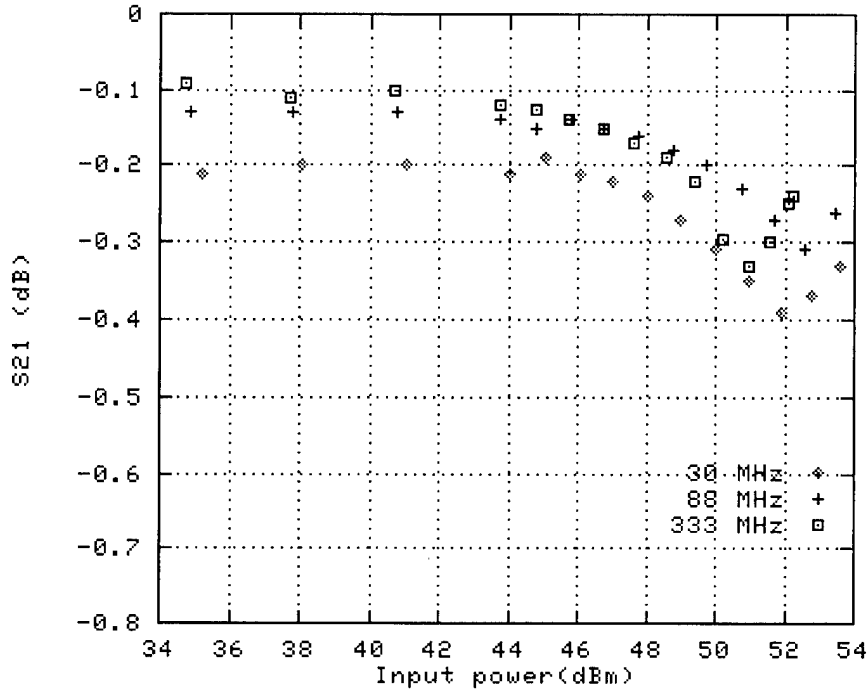


Figure 8. Insertion loss of a PIPINS versus input RF power for three frequencies.

RF standoff voltage was measured with the switch in the OFF-state. The reflected power was monitored (through the third port of the circulator located between the PA and the PIPINS), as was the signal that was capacitively coupled through the PIPINS. A PIPINS can experience self-turn-on (i.e., it will switch from OFF to ON without optical illumination at sufficiently high-incident RF power). Standoff was measured at 333 MHz without self-turn-on. Most measurements were limited (by the PA and loss in the circulator) to 52.5-dBm incident RF power at the device under test. In one case, this power was pushed to 200 W without self-turn-on.

Figure 9 shows hot-switched PIPINS data. The figure plots the envelope of a 300-MHz RF signal versus time.  $P_o = 650$  mW illuminated the PIPINS during the ON-period,  $t_{on} = 50$   $\mu$ s. The repetition period was  $T = 30$  ms. The output voltage was measured across 50  $\Omega$ . The output power during the ON-state was 180 W.

The rise time of a series PIPINS follows the rise time of the optical control signal, in this case, 0.5  $\mu$ s. Its fall time, measured with a fast photodiode, was 0.2  $\mu$ s. When a fast fall time is required and where a ground plane is present, a series-shunt PIPINS circuit can be used. The fast turn-on time of the shunt PIPINS achieves a fast fall time for the switch. Figure 10 shows the rising and falling edges of a hot-switched series-shunt PIPINS. The figure shows a rise time of  $\approx 1$   $\mu$ s and a fall time of  $\approx 2.5$   $\mu$ s. For this measurement,  $P_o = 650$  mW,  $t_{on} = 50$   $\mu$ s,  $T = 90$  ms, and  $P_{rf} = 170$  W at the output.

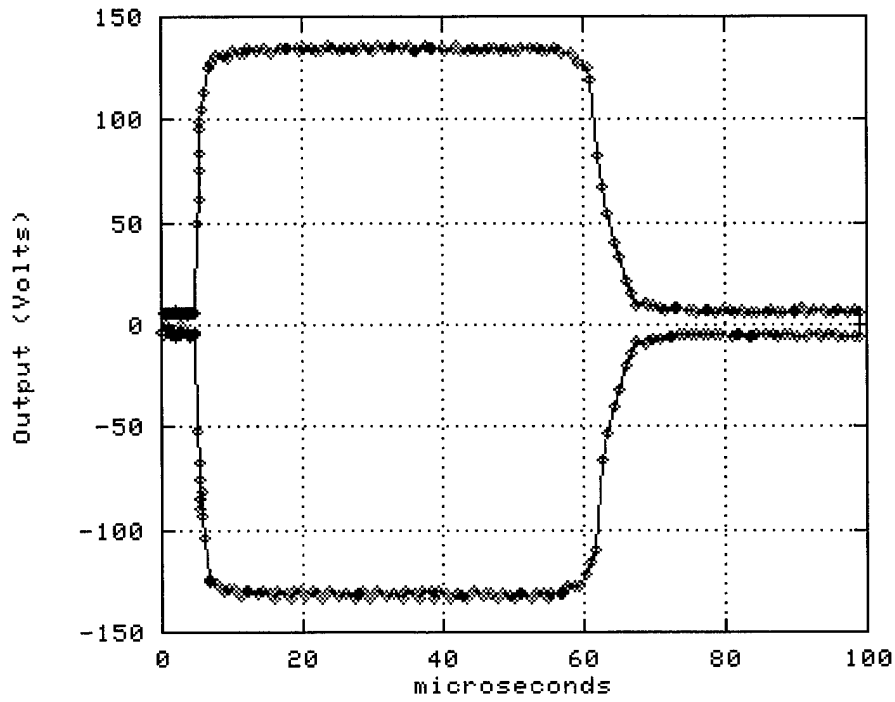


Figure 9. Hot-switched PIPINS output versus time for a 300-MHz signal.

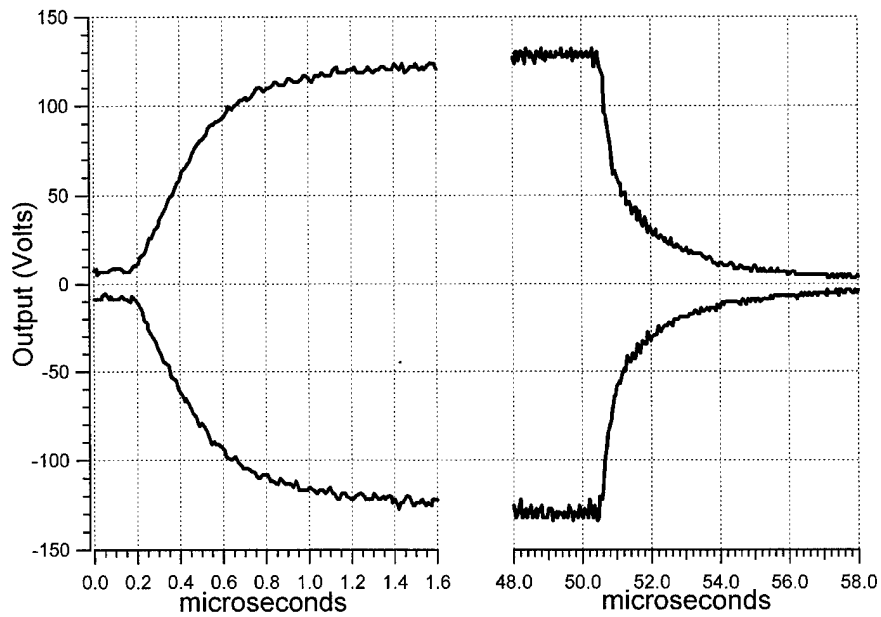


Figure 10. Hot-switched series-shunt PIPINS output (170 W) versus time for a 300-MHz signal (rising and falling edges).

The maximum  $P_{rf}$  that the current PIPINS can handle in hot switching is limited by a latch-on effect (i.e., the switch stays ON after the optical control signal turns OFF). The RF power at latch-on,  $P_{latch}$ , depends on several parameters. For example, figure 11 plots  $P_{latch}$  as a function of the repetition period,  $T$ , when the duty cycle,  $d = t_{on}/T$ , is 50%. The data in figure 10 had a duty cycle considerably less than 50%, allowing higher pulse power operation than figure 11 data.

The linearity in the ON-state of the PIPINS was studied with two-tone intermodulation measurements with up to  $P_{rf} = 50$  W at each fundamental frequency. For the PIPINS made with 100- $\mu$ m-thick diode I regions, with  $P_{rf} = 50$  W at each fundamental ( $f_1 = 44$  MHz and  $f_2 = 49$  MHz), the third-order intermodulation product at 54 MHz was 60 dB below the fundamental. A more detailed description of the PIPINS' high-power switching characteristics appears in Jacobs et al. (2000).

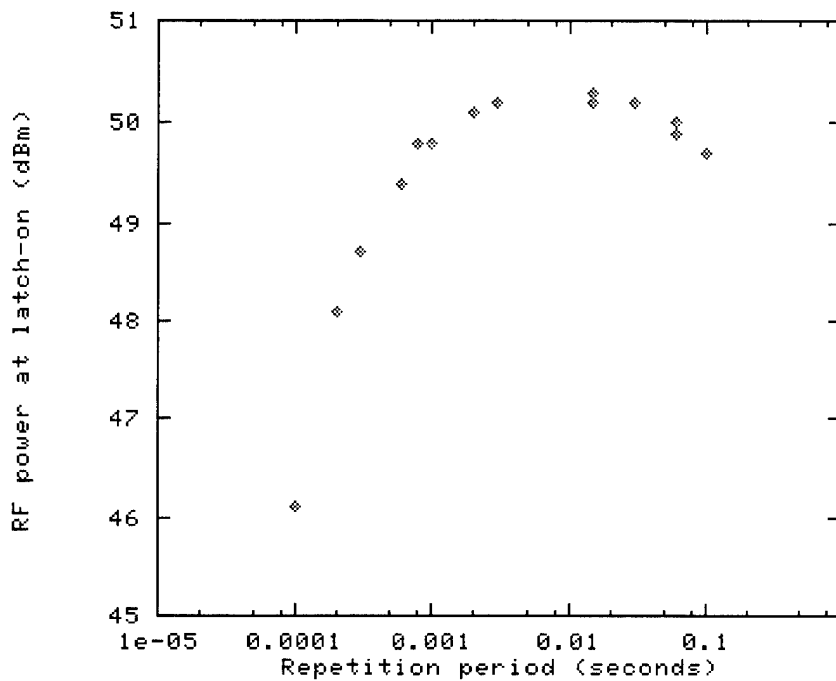


Figure 11. Latch-on power versus repetition period where the duty cycle is 50%.

### 2.2.2 T/R Switch Circuit Development and Demonstration

T/R switch circuit designs were simulated and indicated that the preferred design was a circuit using PIPINS as the OE switching elements. The circuit (figure 12) uses a double series-shunt stage on each arm to reach the required high  $I_s$ . This circuit was assembled and tested up to 100-W cw power. Stray radiation coupling effects within a single package cause degradation of the  $I_s$ . To reduce this degradation, the circuit was assembled and tested with each series-shunt stage in its own package. Each package was connected by SMA connectors. An SMA tee connected the antenna input port to the arms of the switch. The relatively low RF frequencies switched made this modular approach possible.

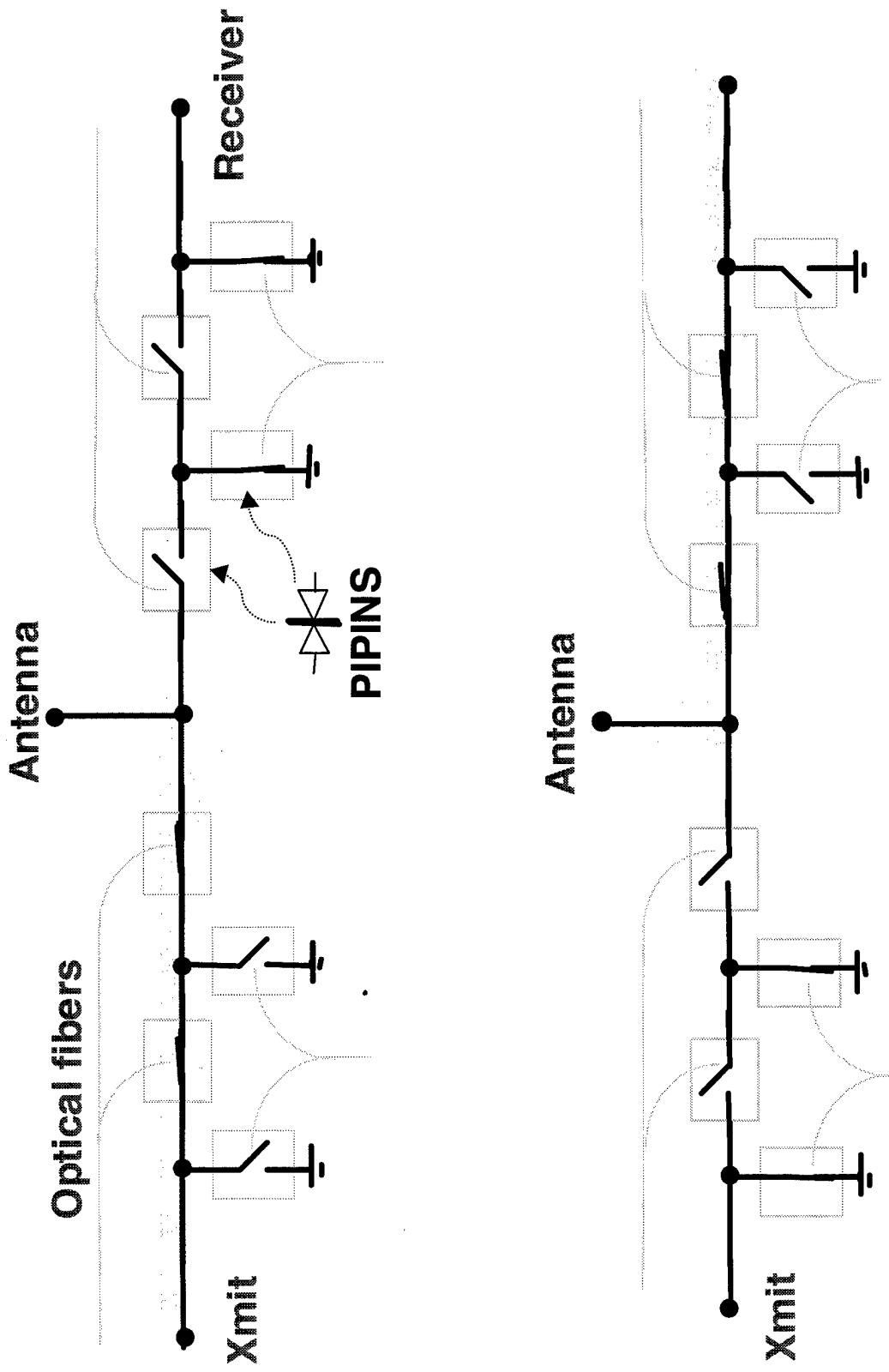


Figure 12. T/R switch circuit design using PIPINS series-shunt switches. Top: transmit mode. Bottom: receive mode.

Figures 13 and 14, respectively, show isolation and insertion loss versus frequency across the VHF band at low RF power (0 dBm). The data in figure 13 were measured after 96 dB of amplification. The  $I_s$  of the switch equals the values on the plot minus an additional 96 dB. This design meets the  $I_s$  goal at low RF power. Data in figure 14 show IL about 0.4 dB over most of the VHF band. The IL starts to increase at the low-frequency end of the curve. This increase might possibly be caused by the sweep out of photogenerated charge carriers. The IL is still better than 0.7 dB at 30 MHz. The switch design can be modified to reduce the IL at the cost of  $I_s$ , which exceeded the goal.

Figure 15 shows insertion loss versus RF power up to 100 W at three frequencies. The low-power IL is supported up to 100 W. Of interest is the high-power 30-MHz data. Degradation in IL (caused by sweep out of photogenerated charge carriers) becomes more likely at lower frequency. This degradation does not occur at powers up to 70 W, the PA power limit available when power was measured.

Figure 16 shows isolation versus RF power up to 100 W for three frequencies, 30 MHz, 100 MHz, and 225 MHz. The transmit arm of the switch was in the ON-state for these measurements.  $I_s$  was measured in the receive arm in the OFF-state. The low-power IL and  $I_s$  were supported up to 100 W. This PIPINS-based T/R switch met the performance goals up to 100 W of dc RF power across the VHF band, showing IL less than 1 dB and  $I_s$  greater than 120 dB.

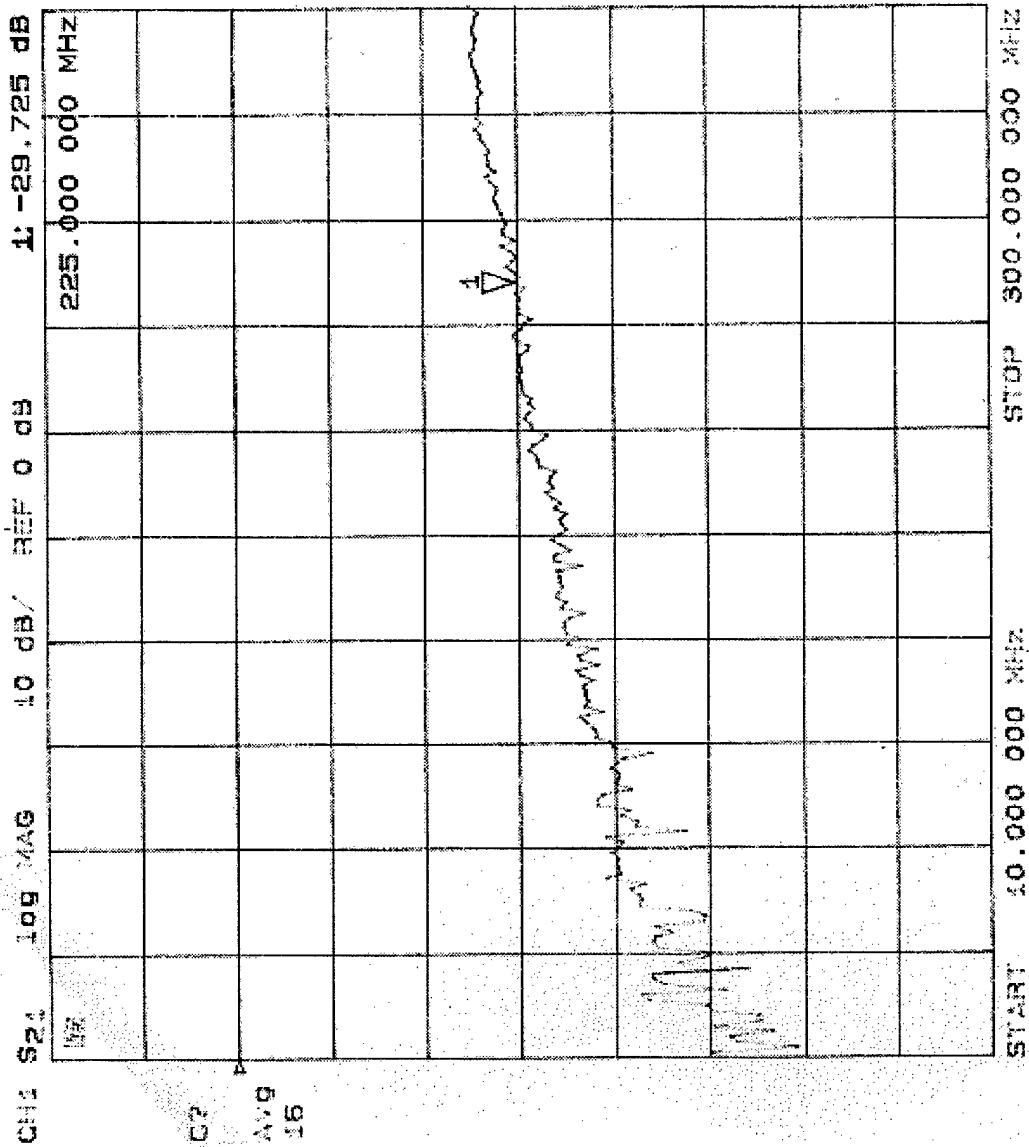


Figure 13. Isolation versus frequency for the switch design in figure 12. The data are recorded after 96 dB of amplification. Therefore, isolation at the 225-MHz marker is -125.725 dB.

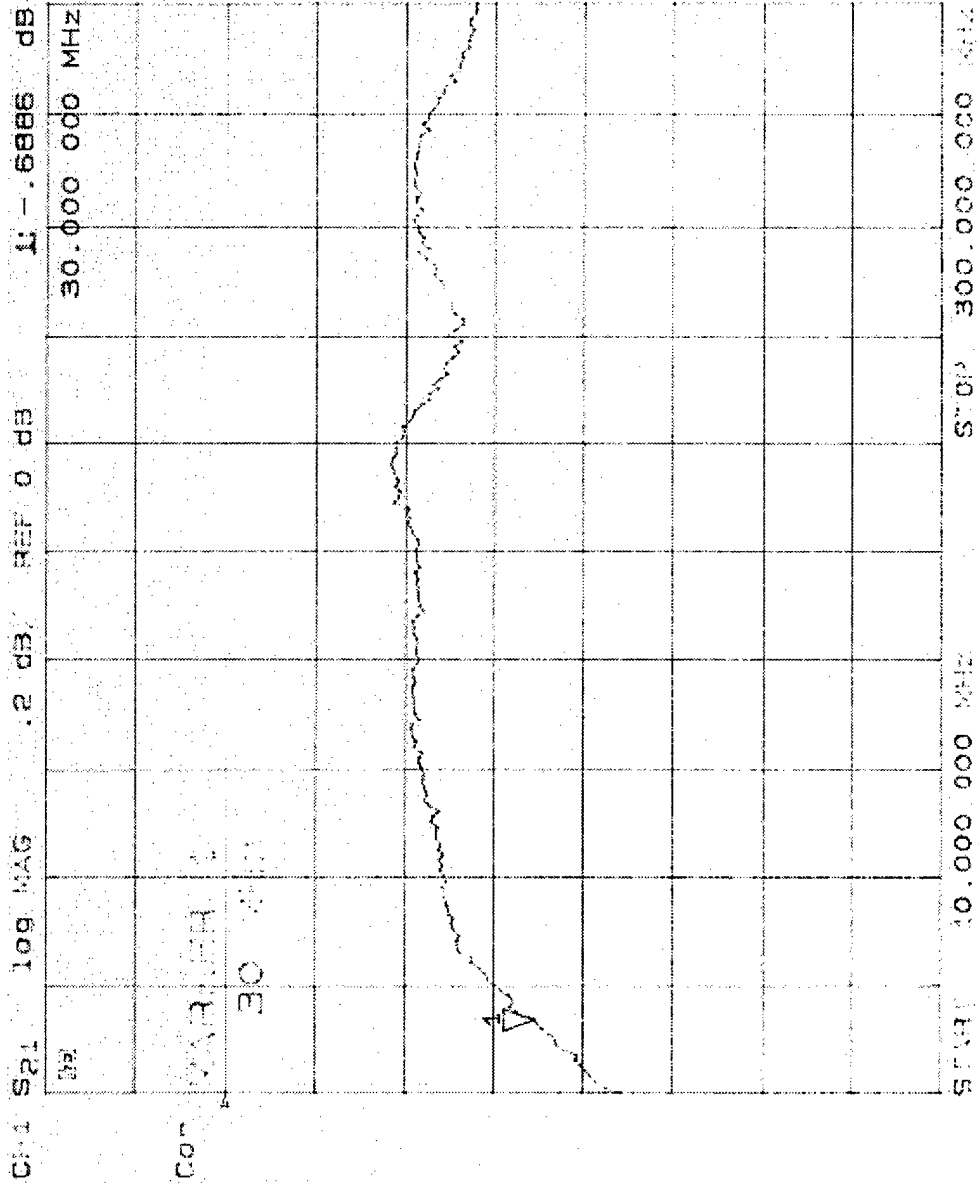


Figure 14. Insertion loss versus frequency for the switch design in figure 12.



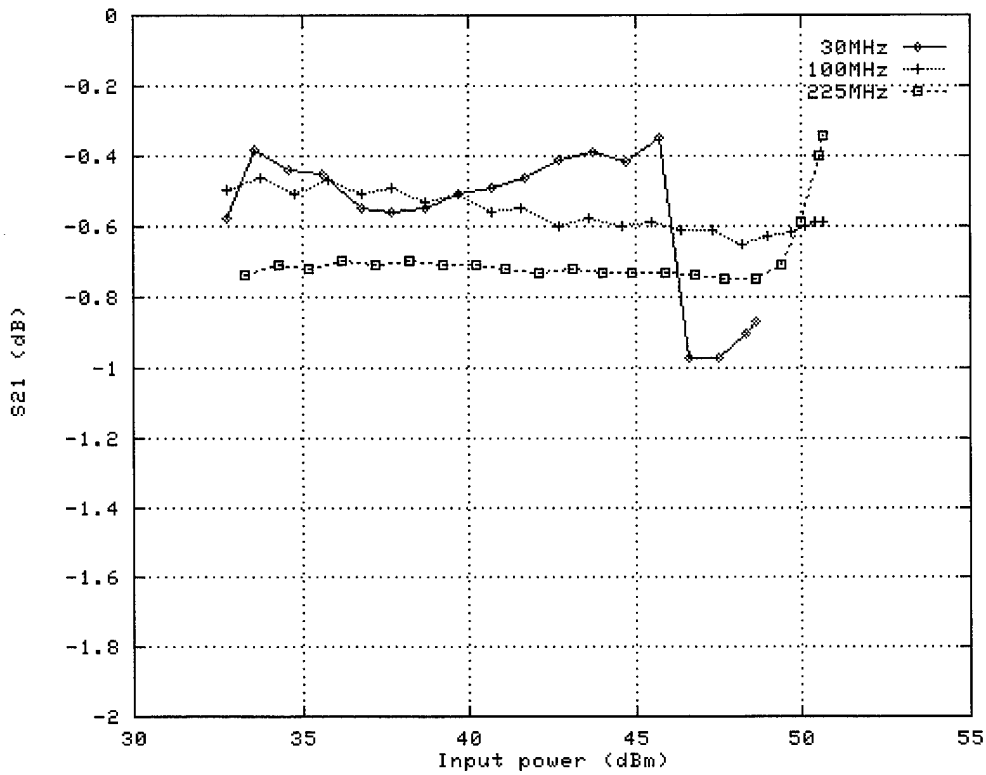


Figure 15. Insertion loss versus RF power at three frequencies for the switch design in figure 12.

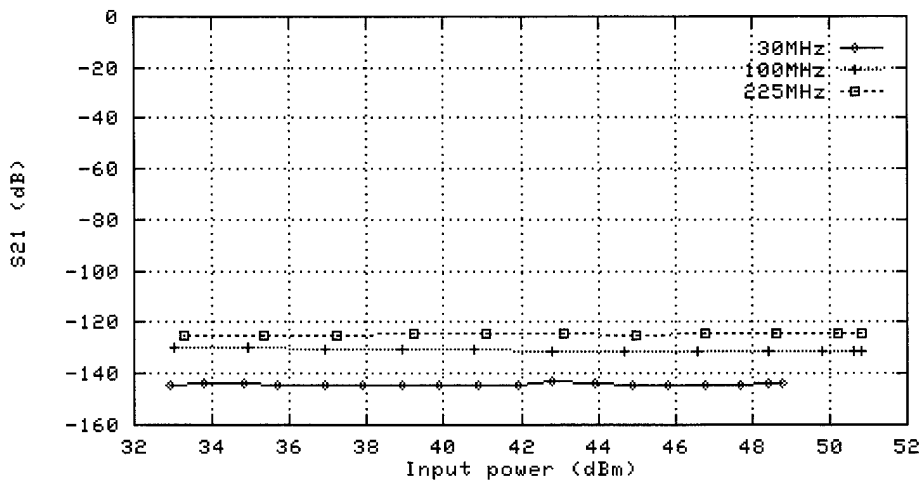


Figure 16. Isolation versus input power for the switch design in figure 12 measured in the OFF-state arm with the other arm in the ON-state.



### 3. SUMMARY

The TST Program developed optically controlled PIN-diode-based RF switches for potential TST applications. These applications included EMI immunity, bias-free operation, switching speed, low noise, power handling, and reliability. An Air Force (CARF) and an Army (TACJAM) system provided performance goals. CARF featured very high ON-OFF ratios at X-band. The ON-OFF ratios were provided by current mechanical switches. TACJAM featured high RF power handling and isolation. For these applications, the TST Program designed, built, and tested switch circuits based upon the PV-PIN switch and the PIPINS. For the CARF case, a PV-PIN circuit yielded suitable isolation, but not insertion loss. The shortfall was caused by inherent semiconductor-based switch properties and microwave packaging techniques. For the TACJAM case, which used a T/R switch, the PIPINS circuit reached the performance goals up to 100-W cw (instrument-limited) across the VHF band. Single PIPINS later handled 200-W cw in cold switching (instrument-limited) and 175-W cw in hot switching, at 30 to 333 MHz.



#### 4. REFERENCES

- Albares, D. J., C. K. Sun, R. Nguyen, and C. T. Chang. 1999. "Optically Controlled RF Switches Combat EMI," *Microwaves & RF* (Apr), pp. 86–98.
- Jacobs, E. W., D. W. Fogliatti, H. Nguyen, D. J. Albares, C. T. Chang, and C. K. Sun. 2001. "Photo-Injection PIN Diode Switch for High Power RF Switching," In press. *IEEE Transactions on Microwave Theory and Techniques*.
- Sun, C. K., R. Nguyen, C. T. Chang, and D. J. Albares. 1996. "Photovoltaic-FET for Optoelectronic RF/ $\mu$ wave Switching," *IEEE Transactions on Microwave Theory and Techniques*, vol. 44, p. 1747.
- Sun, C. K., R. Nguyen, D. J. Albares, and C. T. Chang. 1997. "Photo-Injection Back-to-Back PIN Switch for RF Control," *Electronics Letters*, vol. 33, pp. 1579–1580.
- Sun, C. K., R. Nguyen, and D. J. Albares. 1998. "Photo-Injection Back-to-Back PIN Switch for RF Control." DARPA PSAA-8 Symposium, 13–15 January, Monterey CA.
- Sun, C. K. et al. 1998. "Super High Frequency, High Power Optoelectronic Switch," Patent application submitted, Navy Case No. 78552.
- Sun, C. K., C. T. Chang, R. Nguyen, and D. J. Albares. 1999. "Photovoltaic-p-i-n Diodes for RF Control-Switching Application," *IEEE Transactions on Microwave Theory and Techniques*, vol. 47, p. 2034.





## INITIAL DISTRIBUTION

D0012	Patent Counsel	(1)
D0271	Archive/Stock	(6)
D0274	Library	(2)
D027	M. E. Cathcart	(1)
D0271	E. R. Ratliff	(1)
D0271	D. Richter	(1)
D825	E. W. Jacobs	(20)

Defense Technical Information Center  
Fort Belvoir, VA 22060-6218 (4)

SSC San Diego Liaison Office  
Arlington, VA 22202-4804

Center for Naval Analyses  
Alexandria, VA 22302-0268

Office of Naval Research  
ATTN: NARDIC (Code 362)  
Arlington, VA 22217-5660

Government-Industry Data Exchange  
Program Operations Center  
Corona, CA 91718-8000